Vision Research 159 (2019) 68–75

Contents lists available at ScienceDirect

Vision Research

journal homepage: www.elsevier.com/locate/visres

Altered intra- and inter-regional functional connectivity of the visual cortex in individuals with peripheral vision loss due to retinitis pigmentosa

Han-Dong Dan[a,1], Fu-Qing Zhou[b,1], Xin Huang[a], Yi-Qiao Xing[a], Yin Shen[a,*]

[a] Eye Center, Renmin Hospital of Wuhan University, Wuhan 430060, Hubei, China
[b] Department of Radiology, The First Affiliated Hospital of Nanchang University, Jiangxi Province Medical Imaging Research Institute, Nanchang 330006, Jiangxi, China

ARTICLE INFO

Keywords:
Retinitis pigmentosa
Regional homogeneity
Functional connectivity
Functional magnetic resonance imaging

ABSTRACT

This study investigated changes in intra- and inter-regional functional connectivity (FC) in individuals with retinitis pigmentosa (RP) by using regional homogeneity (ReHo) and FC methods. Sixteen RP individuals and 14 healthy controls (HCs) underwent resting-state functional magnetic resonance imaging scans (fMRI). A combined ReHo and FC method was conducted to evaluate synchronization of brain activity. Compared with HCs, RP individuals had significantly lower ReHo values in the bilateral lingual gyrus/cerebellum posterior lobe (LGG/CPL). In FC analysis, the RP group showed decreased positive FC relative to the HC group, from bilateral LGG/CPL to bilateral LGG/cuneus (CUN) and to left postcentral gyrus (PosCG). In contrast, the RP group showed increased negative FC relative to the HC group, from bilateral LGG/CPL to bilateral thalamus, and decreased negative FC from bilateral LGG/CPL to right middle frontal gyrus (MFG), and to left inferior parietal lobule (IPL). Moreover, ReHo values of the bilateral LGG/CPL showed negative correlations with the duration of RP. FC values of the bilateral LGG/CPL-left IPL showed negative correlations with best-corrected visual acuity (BCVA) of the right eye and left eye in RP individuals. Our results reveal reduced synchronicity of neural activity changes in the primary visual area in RP individuals. Moreover, RP individuals showed intrinsic visual network disconnection and reorganization of the retino-thalamocortical pathway and dorsal visual stream, suggesting impaired visuospatial and stereoscopic vision.

1. Introduction

Visual deprivation may cause experience-dependent plasticity in the human brain. Previous studies have demonstrated functional and morphological reorganization of the visual area in blind individuals (Jiang et al., 2009; Park et al., 2009; Yu et al., 2008). Additionally, plastic changes in auditory, sensorimotor, and language cortices have been associated with blindness (Gizewski, Gasser, de Greiff, Boehm, & Forsting, 2003; Jiang, Stecker, Boynton, & Fine, 2016; Sabbah et al., 2016). Partial blindness also leads to cross-modal plasticity in the human brain. Notably, a retinotopic map exists in the primary visual area (V1). Various neuroimaging studies have demonstrated that peripheral and central vision loss have different patterns of visual processing in the visual area (Burnat, Hu, Kossut, Eysel, & Arckens, 2017; Dilks, Julian, Peli, & Kanwisher, 2014; Masuda et al., 2010). Sabbah et al. reported that individuals with peripheral visual loss showed altered functional connectivity (FC) in V1 (Sabbah et al., 2017). Significantly increased FC between language and visual areas has been found in retinitis pigmentosa (RP) patients with peripheral visual loss and blindness (Sabbah et al., 2016). Cunningham et al. reported that RP patients had significant cross-modal plasticity in the visual cortex (Cunningham, Weiland, Bao, Lopez-Jaime, & Tjan, 2015; Cunningham, Weiland, Bao, & Tjan, 2011). Additionally, Ferreira et al. found that visual cortical remapping was observed in the RP patients (Ferreira et al., 2017). However, it is largely unknown whether peripheral visual loss causes altered intra- and inter-regional FC at rest.

RP individuals provide a unique model to investigate intra- and inter-regional changes in FC following peripheral visual loss. RP is an inherited retinal degeneration characterized by progressive loss of the peripheral visual field (VF). The worldwide prevalence of RP is approximately 1 in 4000 (Hartong, Berson, & Dryja, 2006). Genetic mutations are the primary risk factor for RP (Daiger, Sullivan, & Bowne, 2013); peripheral visual loss in RP occurs as a result of the progressive degeneration of both rod and cone photoreceptor cells. However, thus far, there is a paucity of neuroimaging studies regarding the effects of peripheral visual loss on intra- and inter-regional FC.

* Corresponding author.
E-mail address: yinshen@whu.edu.cn (Y. Shen).
[1] These authors have contributed equally to this work.

https://doi.org/10.1016/j.visres.2019.02.013
Received 21 August 2018; Received in revised form 4 February 2019; Accepted 27 February 2019
Available online 16 April 2019

Synchronous neuronal activities include critical neurophysiological activities, such as information processing, learning, and visual memory (Jutras & Buffalo, 2010; Pipa & Munk, 2011; Sturm & Konig, 2001). Moreover, synchronous neuronal activity of the visual area is closely related to vision (van der Togt, Kalitzin, Spekreijse, Lamme, & Super, 2006). Electroencephalogram and functional magnetic resonance imaging (fMRI) studies have demonstrated that synchronous neural activities are critical in sleep and visual information processing (Diaz, Bassi, Coolen, Vivaldi, & Letelier, 2018; Knyazeva, Fornari, Meuli, Innocenti, & Maeder, 2006). ReHo, a resting-state fMRI technology, is applied to calculate similar time series for a given voxel relative to its nearest neighbors, reflecting the local FC of brain activities (Zang, Jiang, Lu, He, & Tian, 2004). A ReHo map has been evaluated by Kendall's coefficient of concordance (KCC) (Baumgartner, Somorjai, Summers, & Richter, 1999). ReHo is a highly reliable method to reflect neural physiological activities (Zuo et al., 2013). The FC method has been used to investigate a similar time series of two separate brain regions at a long distance from each other (Smith et al., 2017). Previous neuroimaging studies have shown that ReHo and FC could be successfully applied to investigate regional and long-range FC (Han et al., 2018; Liu et al., 2018; Zuo et al., 2017).

Here, we investigated alterations in regional FC, as well as FC between regions with altered ReHo and other brain regions in RP individuals. We assessed whether mean ReHo values and FC values were correlated with best-corrected visual acuity (BCVA), VF, and optical coherence tomography (OCT) findings in RP individuals.

2. Materials and methods

2.1. Subjects

Sixteen right-handed RP individuals and 14 right-handed healthy controls (HCs) participated in this study. The research protocol was approved by the medical ethics committee of the Renmin Hospital of Wuhan University. All data collection and analysis efforts were conducted in accordance with the tenets of the Declaration of Helsinki. All subjects provided informed written consent to participate in the study.

All subjects enrolled in the study met the following criteria: 1) they could undergo scanning by MRI (e.g., they had no cardiac pacemaker or implanted metal device); 2) they had no claustrophobia; 3) they had no heart disease, hypertension, or cerebral disease. High resolution T1-weighted images of all subjects were assessed by an experienced radiologist.

The diagnostic criteria for individuals in the RP group were: 1) presence of night blindness; 2) bone spicule pigmentation of the fundus; retinal vascular stenosis; waxen optic disc (Fig. 1A); and thin retina of OCT (Fig. 1B); 3) peripheral VF loss (Fig. 1C). The exclusion criteria were RP patients with binocular blindness, other related complications (e.g., cataract, glaucoma, or macular edema), secondary RP (e.g., inflammation, trauma, or vascular disease), or surgical history. All HCs met the following criteria: 1) absence of any ocular diseases (e.g., myopia, cataracts, glaucoma, optic neuritis, or retinal degeneration); 2) binocular visual acuity ≥ 1.0; 3) no ocular surgical history; 4) no mental disorders.

2.2. MRI parameters

MRI scanning was performed on a 3-Tesla MR scanner (Discovery MR 750W system; GE Healthcare, Milwaukee, WI, USA) with eight-channel head coil. Whole-brain T1 weights were obtained with magnetization prepared gradient echo image (MPRAGE) with the following parameters: repetition time (TR)/echo time (TE) = 8.5 ms/3.3 ms, thickness = 1.0 mm, no intersection gap, acquisition matrix = 256 × 256, field of view = 240 × 240 mm^2, and flip angle = 12°. Functional images were obtained by using a gradient-echo-planar imaging sequence with the following parameters (TR/TE = 2000 ms/25 ms, thickness = 3.0 mm, gap = 1.2 mm, acquisition matrix = 64 × 64, field of view = 240 × 240 mm^2, flip angle = 90°, voxel size = 3.6 × 3.6 × 3.6 mm^3, and 35 axial). For each subject, 240 volumes were obtained over an 8-minute scanning interval. All subjects underwent MRI scanning with their eyes closed without falling asleep.

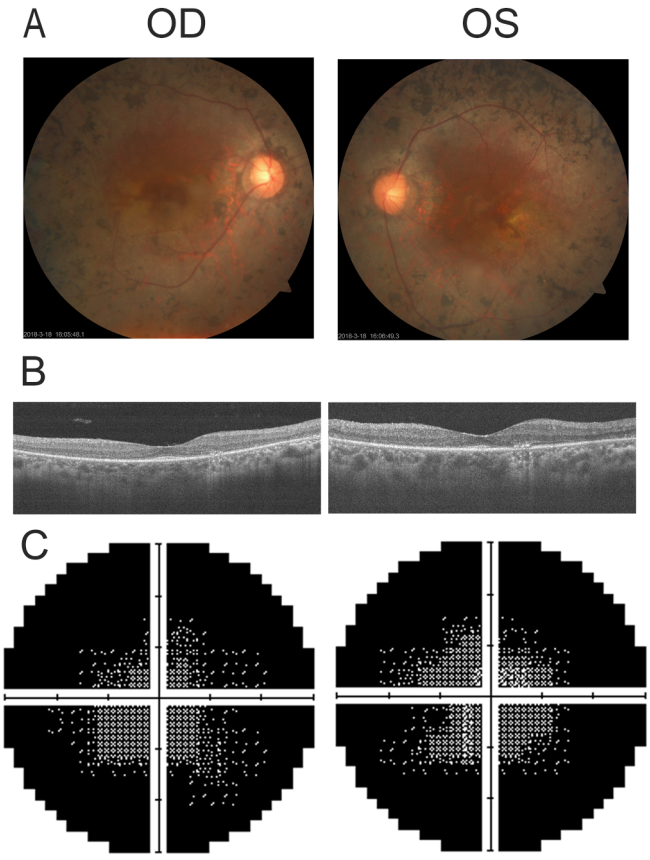

Fig. 1. Typical presentation of retinitis pigmentosa in fundus photographs (A), OCT examination (B), and VF examination (C). *Abbreviations:* OD, oculus dexter; OS, oculus sinister; OCT, optical coherence tomography; VF, visual field.

2.3. fMRI data processing

The DICOM format of the functional images was converted to the NIFTI format using MRIcron software (http://www.cabiatl.com/mricro/mricron/dcm2nii.html). The functional images were preprocessed using Statistical Parametric Mapping SPM12 (http://www.fil.ion.ucl.ac.uk/spm/) and the toolbox for Data Processing Assistant & Analysis for Brain Imaging (http://rfmri.org/dpabi) software implemented in MATLAB 2013a (MathWorks, Natick, MA, USA). Briefly, this included the following steps: (Zang et al., 2004; Zhang, Wang et al., 2016) 1) The first 10 volumes of each subject were discarded due to the signal reaching equilibrium. 2) The remaining 230 volumes of functional BOLD images were corrected for slice timing effects and motion, then realigned. Data from subjects whose head moved > 2 mm or for whom rotation exceeded 2° during scanning were excluded. 3) Individual T1-weighted MPRAGE structural images were registered to the mean fMRI data; resulting aligned T1-weighted images were segmented using the Diffeomorphic Anatomical Registration Through Exponentiated Lie Algebra toolbox to improve spatial precision in the normalization of fMRI data (Goto et al., 2013). Normalized data (in Montreal Neurological Institute 152 space) were re-sliced at a resolution of 3 × 3 × 3 mm^3. 4) Linear regression analysis was used to regress out several covariates (six head motion parameters, mean framewise displacement, global brain signal, and averaged signal from white

matter and cerebrospinal fluid). 5) Finally, data with linear trends were removed, and a temporal band-pass filter was applied (0.01–0.1 Hz).

2.4. Calculation of ReHo

The ReHo index was calculated by REST software (http://www.restfmri.net) (Song et al., 2011). KCC values were assigned to respective voxels by calculating the KCC of a time series of 26 voxels with those of their nearest neighbors, using the following formula where ReHo is the KCC for a given voxel, ranging from 0 to 1 (Zhang, Wang et al., 2016).

$$\mathrm{Re}\,Ho = \frac{\sum (R_i)^2 - n(\bar{R})^2}{K^2(n^3 - n)/12}$$

When the ranked time series is more consistent with its adjacent ones, the KCC value is closer to 1; k is the voxel number of the time series (in our study, k = 27, comprising a given voxel that was located in the cubic center and its adjacent 26 voxels); n is the number of ranks; Ri is the sum rank of the ith time point; and ReHo maps were constructed by dividing the KCC of each voxel by the averaged KCC of the whole brain. All ReHo maps of each voxel were z-transformed with Fisher's r-to-z transformation to reduce the influence of individual variation for group statistical comparisons. The remaining z ReHo maps were spatially smoothed with a Gaussian kernel of $4 \times 4 \times 4\,mm^3$ full width at half maximum.

2.5. Seed-based FC analysis

FC analysis was performed using REST software. Brain regions with significantly different ReHo were defined as regions of interest, each of which had a 10-mm radius around the coordinates (x = 0, y = −69, z = −3). Correlation analysis throughout the time course was performed between the spherical seed region and each voxel of the whole brain for each subject. Subsequently, all FC maps were z-transformed with Fisher's r-to-z transformation to reduce the influence of individual variation for group statistical comparisons.

2.6. Ophthalmic testing

Visual function testing: the visual acuity of all subjects was measured by applying the decimal view chart. The VF of RP individuals was measured using the Humphrey HFA II-750 (Carl Zeiss Meditec AG, Jena, Germany). OCT and fundus photograph testing: The mean retinal nerve fiber layer thickness of RP individuals was calculated by using spectral domain OCT angiography (AngioVue®, Optovue, CA, USA). High resolution fundal photographs of RP individuals were obtained with a digital fundus camera (VISUCAM, Carl Zeiss Meditec AG).

2.7. Statistical analysis

The chi-squared test was used for sex comparisons between the groups. An independent-samples *t*-test was used for age, weight, and BCVA comparisons between the groups, using SPSS version 20.0 software (SPSS Inc., Chicago, IL, USA). Intra-group patterns in ReHo maps were analyzed using the one-sample *t*-test with SPM12 software (voxel-level $P < 0.001$, Gaussian random field [GRF] correction, cluster-level $P < 0.05$). A two-sample *t*-test was applied to compare group differences in the zReHo maps and zFC maps, using the GRF method to correct for multiple comparisons and regressed covariates of age and sex with SPM12 software (two-tailed, voxel-level $P < 0.01$, GRF correction, cluster-level $P < 0.05$). The Pearson correlation coefficient was applied to assess relationships between zReHo values and zFC values of different brain regions and visual measurement data using SPSS version 20.0 software (SPSS Inc.).

Table 1
Demographics and visual measurements between RP and HC groups.

	RP group	HC group	T-values	P-values
Gender (male/female)	11/5	6/8	2.039	0.153
Age (years)	35.56 ± 13.25	40.57 ± 11.48	−1.098	0.281
Weight (kg)	65.43 ± 6.43	67.35 ± 5.94	−0.845	0.405
Handedness	16R	14R	N/A	N/A
Course (years)	18.93 ± 10.54	N/A	N/A	N/A
BCVA-OD	0.44 ± 0.32	1.20 ± 0.21	−7.441	< 0.001
BCVA-OS	0.51 ± 0.35	1.14 ± 0.23	−5.821	< 0.001
mRNFL thickness -OD (μm)	218.31 ± 43.70	N/A	N/A	N/A
mRNFL thickness -OS (μm)	214.56 ± 42.94	N/A	N/A	N/A
VF(MD)-OD (dB)	26.87 ± 3.37	N/A	N/A	N/A
VF(MD)-OS (dB)	27.19 ± 3.21	N/A	N/A	N/A

Note: Data presented as mean ± standard deviation, Chi-square test was used for gender comparisons. Independent sample *t*-test was used for age and weight and BCVA comparisons.
Abbreviations: RP, retinitis pigmentosa; HC, health control; BCVA, best corrected visual acuity; R, right; OD, oculus dexter; OS, oculus sinister; mRNFL, mean retinal nerve fibre layer; MD, mean deficit; VF, visual field; N/A, not applicable.

3. Results

3.1. Demographics and visual measurements

There were significant differences in BCVA in the right eye ($P < 0.001$) and BCVA in the left eye ($P < 0.001$). There were no significant differences in sex, age, or weight between the groups (Fig. 1 and Table 1).

3.2. ReHo analysis

The spatial distribution of ReHo maps of the RP individuals and HCs appeared to be similar. However, RP patients showed markedly lower ReHo values in the visual area, compared with those of the HCs (Fig. 2A and B). Compared with those of the HCs, RP individuals showed significantly lower ReHo values in the bilateral lingual gyrus/cerebellum posterior lobe (LGG/CPL) (Brodmann area [BA] 17, 18[2]) (Fig. 3A [blue] and Table 2) (two-tailed, voxel-level $P < 0.01$, GRF correction, cluster-level $P < 0.05$). The altered mean ReHo values of bilateral LGG/CPL between two groups are shown in a histogram (Fig. 3B).

3.3. FC analysis

The RP group showed decreased positive FC between the bilateral LGG/CPL and bilateral LGG/cuneus (CUN), and to left postcentral gyrus (PosCG), relative to that observed in the HC group (voxel-level $P < 0.01$, GRF correction, cluster-level $P < 0.05$) (Fig. 4A and Table 3). Furthermore, the RP group showed increased negative FC between the bilateral LGG/CPL and bilateral thalamus, as well as decreased negative FC between the bilateral LGG/CPL and right middle frontal gyrus (MFG), and to left inferior parietal lobule (IPL), relative to that observed in the HC group (voxel-level $P < 0.01$, without correction) (Fig. 4B and Table 3). The altered mean FC values for several brain regions between the two groups are shown in a histogram (Fig. 4C and D, and Table 3).

[2] Brodmann area 17, 18, 19: primary visual cortex that processes visual information; Brodmann area 3: primary somatosensory cortex that processes a variety of sensory input; Brodmann area 4: primary motor cortex that controls motor output; Brodmann area 8, 9: middle frontal gyrus that processes higher cognition function; Brodmann area 40: inferior parietal lobule that processes the vision-motor function.

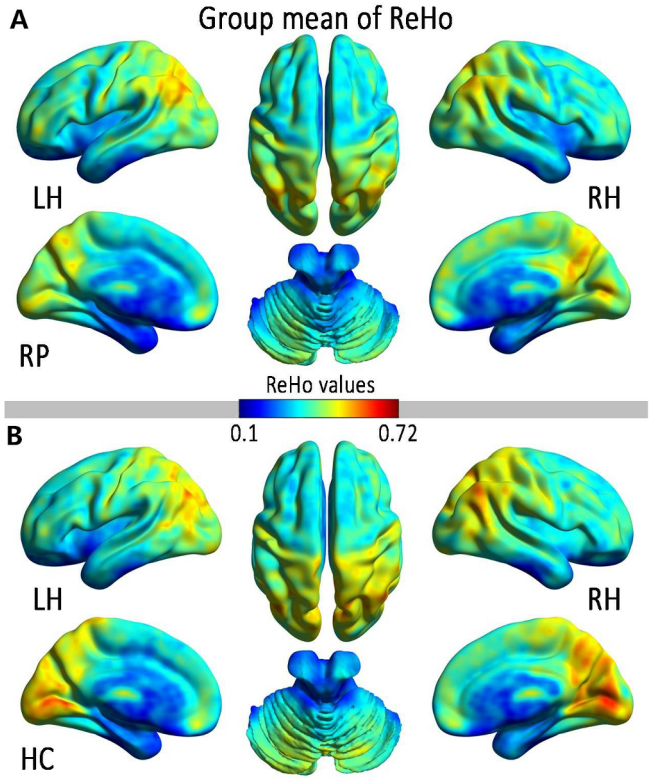

Fig. 2. Distribution pattern of ReHo at the group level for RP and HC subjects in the typical frequency band (0.01–0.1 Hz). *Note:* Within-group indicates ReHo maps in RP individuals (A) and HCs (B) (voxel-level P < 0.01, GRF correction). *Abbreviations:* ReHo, regional homogeneity; RP, retinitis pigmentosa; HC, healthy control; LH, left hemisphere; RH, right hemisphere; GRF, Gaussian random field.

3.4. Correlation analysis

ReHo values of the bilateral LGG/CPL showed negative correlations with the duration of RP ($r = -0.550$, $p = 0.027$). FC values of the bilateral LGG/CPL-left IPL showed negative correlations with BCVA in the right eye ($r = -0.547$, $p = 0.028$) and BCVA in the left eye ($r = -0.627$, $p = 0.009$) in RP individuals (Fig. 5A–C).

Table 2
Significant differences in the ReHo between two groups.

Brain regions	BA	T-Peak scores (P-values)	MNI coordinates (x, y, z)	Cluster size (voxels)
Bilateral LGG/CPL	17, 18	−5.12, (< 0.01)	0,-69, −3	498

Note: The statistical threshold was set at the voxel level with p < 0.01 for multiple comparisons using Gaussian random-field theory (two-tailed, voxel-level P < 0.01, GRF correction, cluster-level P < 0.05).
Abbreviations: ReHo, regional homogeneity; BA, Brodmann area; RP, retinitis pigmentosa; HC, health control; MNI, Montreal Neurological Institute; GRF, Gaussian random field; LGG, Lingual Gyrus; CPL, Cerebellum Posterior Lobe.

4. Discussion

To the best of our knowledge, our study is the first to reveal altered intra- and inter-regional FC in individuals with peripheral vision loss. Our results showed that RP individuals exhibit significantly lower ReHo values in the bilateral LGG/CPL (BA 17, 18), compared with ReHo values of HCs. Moreover, the RP group exhibited significantly decreased positive FC, relative to that in the HC group, from bilateral LGG/CPL to bilateral LGG/CUN (BA 17, 18, 19) and to left PosCG (BA 3, 4). In contrast, the RP group exhibited significantly increased negative FC relative to that in the HC group, from bilateral LGG/CPL to bilateral thalamus, and significantly decreased negative FC from bilateral LGG/CPL to right MFG (BA 8, 9), as well as to left IPL (BA 40). Furthermore, ReHo values of the bilateral LGG/CPL showed negative correlations with the duration of RP. FC values of the bilateral LGG/CPL-left IPL showed negative correlations with BCVA in the right eye and BCVA in the left eye in RP individuals.

RP individuals showed lower ReHo values in the bilateral LGG/CPL (BA 17, 18). The LGG is the location of V1, which receives visual signals from the retina. These visual signals are transmitted to higher visual cortical areas via ventral and dorsal visual pathways; neural activity in V1 is closely related to visual function (Kagan, Gur, & Snodderly, 2008). Notably, retinal lesions lead to the reorganization of V1 (Botelho, Ceriatte, Soares, Gattass, & Fiorani, 2014); in a task fMRI study, an

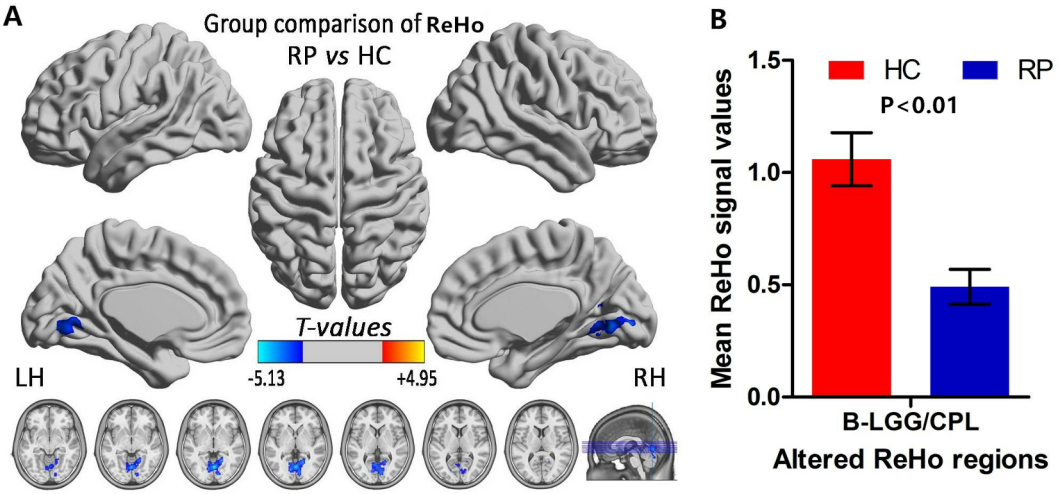

Fig. 3. Comparisons of ReHo between RP and HC groups. Note: Significant regional spontaneous activity differences were found between the two groups. (A) Blue areas indicate lower ReHo values (two-tailed, voxel-level P < 0.01, GRF correction, cluster-level P < 0.05). (B) Altered mean ReHo values between RP and HC groups are shown in the histogram. *Abbreviations:* ReHo, regional homogeneity; RP, retinitis pigmentosa; HC, healthy control; LH, left hemisphere; RH, right hemisphere; LGG, lingual gyrus; CPL, cerebellum posterior lobe; B, bilateral; GRF, Gaussian random field. (For interpretation of the references to color in this figure legend, the reader is referred to the web version of this article.)

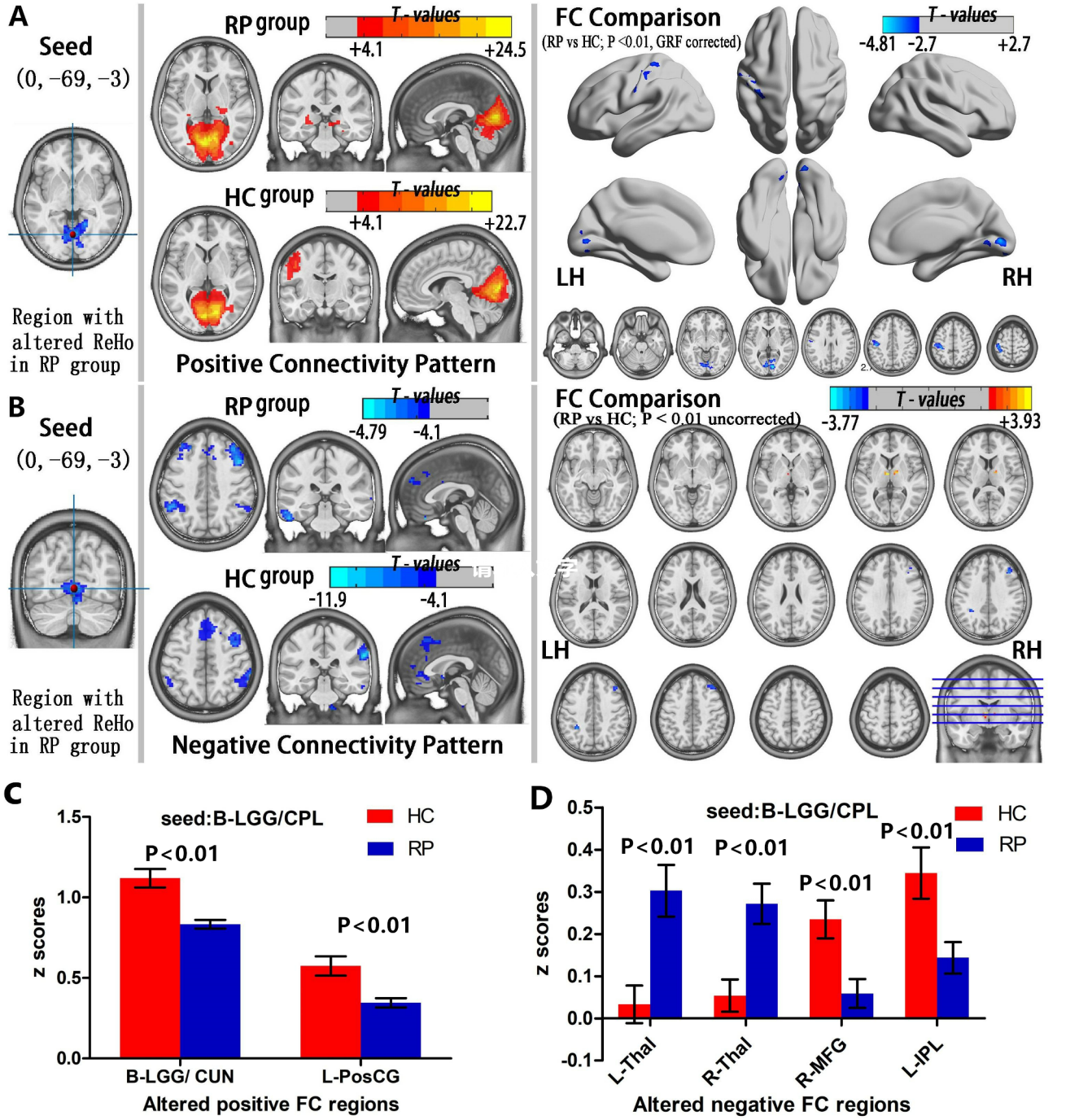

Fig. 4. Comparisons of seed-based FC-altered ReHo between RP and HC groups. *Note:* Significant seed-based functional connectivity activity differences were found between the two groups. Positive connectivity pattern (A) (voxel-level P < 0.01, GRF correction, cluster-level P < 0.05) and negative connectivity pattern (B) (voxel-level P < 0.01, without correction), demonstrating differences in FC between the two groups. Color bars indicate T-values. (C and D) Altered mean positive FC and negative FC values between RP and HC groups are shown in the histogram. *Abbreviations:* ReHo, regional homogeneity; RP, retinitis pigmentosa; HC, healthy control; FC, functional connectivity; LH, left hemisphere; RH, right hemisphere; GRF, Gaussian random field; LGG, lingual gyrus; CPL, cerebellum posterior lobe; CUN, cuneus; PosCG, postcentral gyrus; Thal, thalamus; MFG, middle frontal gyrus; IPL, inferior parietal lobule.

unresponsive lesion projection zone in V1 was observed in RP individuals (Masuda et al., 2010). RP is associated with aggressive atrophy of rod photoreceptor cells, which may lead to altered neural activity in V1 due to reduction of retinal signal input (Wong & Kwok, 2016). Furthermore, various studies have revealed that RP individuals exhibit abnormal structures in the visual pathway and V1. Machado et al. observed reduced gray matter volume in V1 in RP individuals (Rita Machado et al., 2017). Several diffusion tensor imaging (DTI) studies have revealed that RP individuals show lower fractional anisotropy in the optic nerve and optic radiation (Ohno et al., 2015; Zhang, Guo et al., 2016). Thus, reduced retinal input and functional and morphological changes in V1 might contribute to the decreased ReHo values observed in the V1 in RP individuals in the present study. RP patients might exhibit transsynaptic degeneration; degenerating axons originate from the retinal ganglion cell death of directly connected neurons, and this degeneration propagates toward more posterior parts of the visual pathways, eventually involving the visual cortex. Furthermore, ReHo values of the bilateral LGG/CPL showed negative

Table 3
Comparison of FC values seed as the altered ReHo regions between two groups.

Condition	Brain regions	BA	Peak T scores, (p-values)	MNI coordinates (x, y, z)	Cluster size (voxels)
ROI in bilateral LGG/CPL with significant positive connectivity pattern (voxel-level P < 0.01, GRF correction, cluster-level P < 0.05)					
RP < HC	Bilateral Lingual Gyrus/ Cuneus	17,18,19	−4.80, (< 0.01)	12,-84, 3	391
RP < HC	Left Postcentral Gyrus	3, 4	−4.135,(< 0.01)	−48,-21, 39	306
ROI in bilateral LGG/CPL with significant negative connectivity pattern (voxel-level P < 0.01, without correction)					
RP > HC	Left Thalamus	–	3.814, (< 0.01)	−3, −9, 6	11
RP > HC	Right Thalamus	–	3.657, (< 0.01)	15, −6,6	14
RP < HC	Right Middle Frontal Gyrus	8, 9	−3.013,(< 0.01)	39, 27, 36	37
RP < HC	Left Inferior Parietal Lobule	40	−3.040,(< 0.01)	−33, −48,39	11

Note: The statistical threshold was set at the voxel level with p < 0.01 for multiple comparisons using Gaussian random-field theory.
Abbreviations: FC, functional connectivity; ReHo, regional homogeneity; ROI, region of interest; LGG, Lingual Gyrus; CPL, cerebellum posterior lobe; BA, Brodmann area; RP, retinitis pigmentosa; HC, health control; MNI, Montreal Neurological Institute; GRF, Gaussian random field.

correlations with the duration of RP, indicating that compensation for V1 may occur in late stages of the disease.

In FC analysis, the RP group exhibited significantly decreased positive FC between the bilateral LGG/CPL (BA 17, 18) and bilateral LGG/CUN (BA 17, 18, 19), relative to that in the HC group. Wang et al. reported that spontaneous activity of the V1 visual association areas (cuneus and precuneus) occurred at rest in sighted subjects (Wang et al., 2008). Visual signals are processed in the visual stream, following top-down modulations through feedback connections; these connections between contribute to comprehension of the visual scene. In contrast, blind individuals showed decreased FC within the visual area, relative to that observed in sighted subjects (Liu et al., 2007). Reduced FC within the visual network was also present in patients with primary open-angle glaucoma (Wang et al., 2017). RP individuals were characterized by peripheral vision loss, leading to reduced retinal signal input to V1. Thus, we speculated that reduced retinal input might lead to reduced positive FC within the visual cortex, indicating abnormal top-down modulation in RP patients. Significantly decreased positive FC between the bilateral LGG/CPL (BA 17, 18) and left PosCG (BA 3, 4) was observed in RP individuals, relative to that in HCs. In particular, PosCG is the location of the primary somatosensory cortex (S1), which is involved in touch and pain sensation (Ploner, Schmitz, Freund, & Schnitzler, 2000). S1 also plays a critical role in visual processing in the visual-tactile system (Rossetti, Miniussi, Maravita, & Bolognini, 2012). We speculate that reduced visual input might lead to reduced FC between the V1 and somatosensory cortices in RP individuals. Nir et al. demonstrated that spontaneous neural fluctuations in S1 were significantly correlated with V1 activity in sighted subjects (Nir, Hasson, Levy, Yeshurun, & Malach, 2006). Moreover, Yu et al. demonstrated that reduced FC between the left V1 and the precentral gyri was present in early blindness (Yu et al., 2008). Furthermore, reduced visual input might reflect cross-modal plasticity in the V1. Reduced positive FC between the bilateral LGG/CPL (BA 17, 18) and left PosCG (BA 3, 4) was observed in RP individuals, reflecting cross-modal plasticity in S1 due to the loss of visual signal input in RP individuals.

The RP group showed significantly increased negative FC between the bilateral LGG/CPL (BA 17, 18) and bilateral thalamus, relative to that in the HC group. Negative FC comprises spontaneous BOLD signals in two brain regions with a negative Pearson cross-correlation coefficient (also known as an anticorrelation). Negative FC may result in phase delay of synchronous signals along the shortest path in large-scale brain functional networks. The thalamus is a crucial relay that transfers various afferents from multiple sensory organs to the primary sensory cortex. The lateral geniculate nucleus (LGN) is the portion of the thalamus that transfers visual signals to the V1 through the retino-thalamocortical pathway (Bhattacharya, Bond, O'Hare, Turner, & Durrant, 2016; Nakamura, 2018; Neuenschwander, Castelo-Branco, Baron, & Singer, 2002). Visual responses in the retina and LGN exhibit oscillatory patterning within a broad range of frequencies (Neuenschwander et al., 2002; Neuenschwander & Singer, 1996). Notably, Hernowo et al. reported that patients with primary open-angle glaucoma showed grey matter volume atrophy in the retino-thalamocortical pathway (Hernowo, Boucard, Jansonius, Hooymans, & Cornelissen, 2011). Ptito et al. demonstrated that abnormalities in the structure of retino-thalamocortical pathway were observed in patients with congenital blindness (Ptito, Schneider, Paulson, & Kupers, 2008). A previous animal study demonstrated an association between early blindness and abnormal thalamocortical connections (Karlen, Kahn, & Krubitzer, 2006). Furthermore, a DTI study revealed that blind individuals exhibited significant alterations in thalamic microstructure (Reislev et al., 2017). These findings provide converging evidence that visual deprivation (peripheral vision loss) might be associated with dysfunction of the retino-thalamocortical pathway. Degeneration of rod photoreceptor cells leads to reduced visual signal input in the LGN of RP individuals, which may affect FC between the thalamus and V1. Thus, our results suggests that RP might lead to dysfunctional connections in the retino-thalamocortical pathway.

The RP group showed reduced negative FC between the bilateral LGG/CPL (BA 17, 18) and left IPL (BA 40), relative to that in the HC group. The IPL is the core hub of the dorsal visual stream, which is involved in visuospatial representation and visual word recognition (Crottaz-Herbette, Fornari, & Clarke, 2014; Rizzolatti & Matelli, 2003; Sliwinska, James, & Devlin, 2015). The IPL also plays an important role in stereoscopic depth perception (Backus, Fleet, Parker, & Heeger, 2001). Thus, we speculated that reduced negative FC between the bilateral LGG/CPL and IPL might explain the impaired visuospatial and stereoscopic vision observed in RP individuals. Moreover, the FC values of the bilateral LGG/CPL-left IPL showed negative correlations with BCVA in the right eye and BCVA in the left eye in RP individuals. Visual acuity is correlated with visuospatial and stereoscopic vision in the RP group. Thus, reorganization of the dorsal visual stream may occur in RP individuals.

There were several limitations in our study. First, the study involved a small group of subjects. Second, although all subjects underwent fMRI scanning without any task, ReHo and FC signals were likely to be affected by physiological noise (i.e., by cardiac and respiratory activity). In a future study, we will enlarge the sample size. Multimodal MRI imaging technologies will be applied to further investigate the neural plasticity in individuals with peripheral vision loss.

5. Conclusions

Our results highlight reduced synchronicity of neural activities in the V1 in individuals with RP. Moreover, RP individuals showed intrinsic visual network disconnection and reorganization of the retino-thalamocortical pathway and dorsal visual stream, which suggest impaired visuospatial and stereoscopic vision in these individuals. These findings offer an opportunity to better understand the underlying neural mechanism of peripheral vision loss in RP.

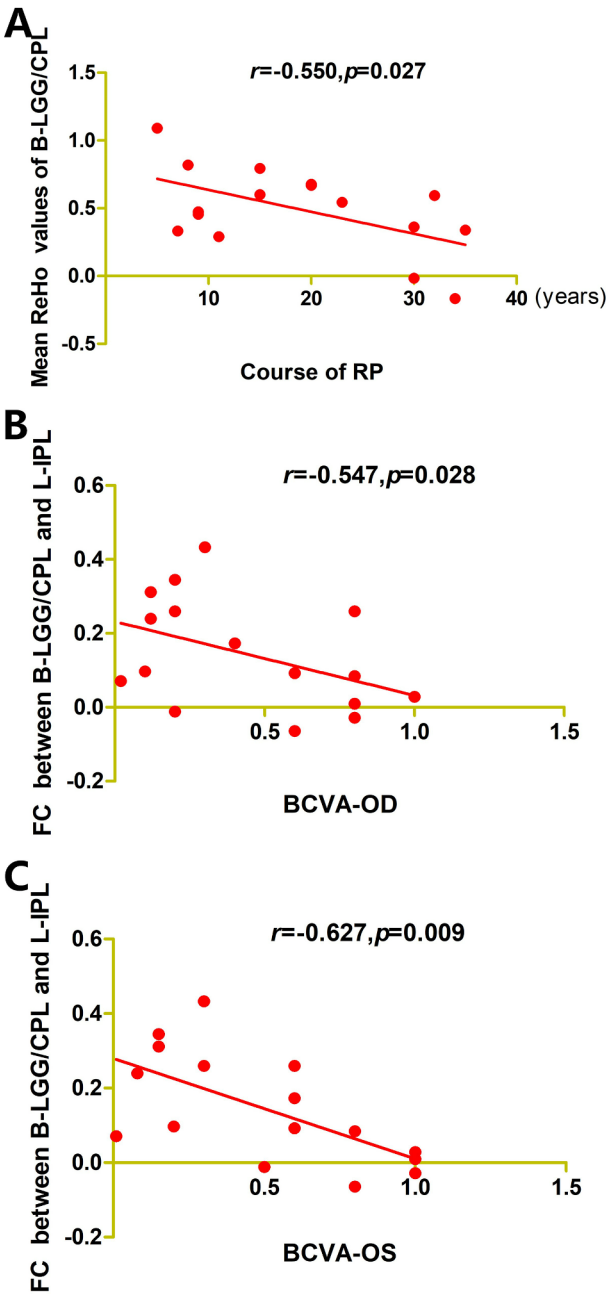

Fig. 5. A significant negative correlation was observed between ReHo of the BGG/CPL and the duration of RP. (A) A significant negative correlation was observed between the FC of the L-IPL and BCVA in the right eye (B) and BCVA in the left eye (C) in RP individuals. *Abbreviations:* ReHo, regional homogeneity; RP, retinitis pigmentosa; FC, function connectivity; LGG, lingual gyrus; CPL, cerebellum posterior lobe; BCVA, best-corrected visual acuity; OD, oculus dexter; OS, oculus sinister; B, bilateral; L, left; IPL, inferior parietal lobule.

Conflicts of interest

The authors declare that they have no conflict of interest with regard to this work.

Funding

This study was supported by the National Natural Science Foundation of China (Grant No. 81470628) and the International Science & Technology Cooperation Program of China (2017YFE0103400).

Acknowledgments

The authors would like to thank all the subjects who participated in this study.

Ethics approval and consent to participate

The research protocol was approved by the medical ethics committee of the Renmin Hospital of Wuhan University. All data collection and analysis efforts were conducted in accordance with the tenets of the Declaration of Helsinki. All subjects were given an informed written consent form.

Consent for publication

Not applicable.

References

Backus, B. T., Fleet, D. J., Parker, A. J., & Heeger, D. J. (2001). Human cortical activity correlates with stereoscopic depth perception. *Journal of Neurophysiology, 86*(4), 2054–2068.

Baumgartner, R., Somorjai, R., Summers, R., & Richter, W. (1999). Assessment of cluster homogeneity in fMRI data using Kendall's coefficient of concordance. *Magnetic Resonance Imaging, 17*(10), 1525–1532.

Bhattacharya, B. S., Bond, T. P., O'Hare, L., Turner, D., & Durrant, S. J. (2016). Causal role of thalamic interneurons in brain state transitions: A study using a neural mass model implementing synaptic kinetics. *Frontiers in Computational Neuroscience, 10*, 115.

Botelho, E. P., Ceriatte, C., Soares, J. G., Gattass, R., & Fiorani, M. (2014). Quantification of early stages of cortical reorganization of the topographic map of V1 following retinal lesions in monkeys. *Cerebral Cortex, 24*(1), 1–16.

Burnat, K., Hu, T. T., Kossut, M., Eysel, U. T., & Arckens, L. (2017). Plasticity beyond V1: Reinforcement of motion perception upon binocular central retinal lesions in adulthood. *Journal of Neuroscience, 37*(37), 8989–8999.

Crottaz-Herbette, S., Fornari, E., & Clarke, S. (2014). Prismatic adaptation changes visuospatial representation in the inferior parietal lobule. *Journal of Neuroscience, 34*(35), 11803–11811.

Cunningham, S. I., Weiland, J. D., Bao, P., Lopez-Jaime, G. R., & Tjan, B. S. (2015). Correlation of vision loss with tactile-evoked V1 responses in retinitis pigmentosa. *Vision Research, 111*(Pt B), 197–207.

Cunningham, S. I., Weiland, J. D., Bao, P., & Tjan, B. S. (2011). Visual cortex activation induced by tactile stimulation in late-blind individuals with retinitis pigmentosa. *Conference proceedings: Annual International Conference of the IEEE Engineering in Medicine and Biology Society, 2011*, 2841–2844.

Daiger, S. P., Sullivan, L. S., & Bowne, S. J. (2013). Genes and mutations causing retinitis pigmentosa. *Clinical Genetics, 84*(2), 132–141.

Diaz, J., Bassi, A., Coolen, A., Vivaldi, E. A., & Letelier, J. C. (2018). Envelope analysis links oscillatory and arrhythmic EEG activities to two types of neuronal synchronization. *Neuroimage, 172*, 575–585.

Dilks, D. D., Julian, J. B., Peli, E., & Kanwisher, N. (2014). Reorganization of visual processing in age-related macular degeneration depends on foveal loss. *Optometry and Vision Science, 91*(8), e199–206.

Ferreira, S., Pereira, A. C., Quendera, B., Reis, A., Silva, E. D., & Castelo-Branco, M. (2017). Primary visual cortical remapping in patients with inherited peripheral retinal degeneration. *NeuroImage: Clinical, 13*, 428–438.

Gizewski, E. R., Gasser, T., de Greiff, A., Boehm, A., & Forsting, M. (2003). Cross-modal plasticity for sensory and motor activation patterns in blind subjects. *Neuroimage, 19*(3), 968–975.

Goto, M., Abe, O., Aoki, S., Hayashi, N., Miyati, T., Takao, H., et al. (2013). Diffeomorphic Anatomical Registration Through Exponentiated Lie Algebra provides reduced effect of scanner for cortex volumetry with atlas-based method in healthy subjects. *Neuroradiology, 55*(7), 869–875.

Han, W., Qian, S., Jiang, Q., Liu, K., Li, B., & Sun, G. (2018). Regional and long-range neural synchronization abnormality during passive hyperthermia. *Behavioural Brain Research, 341*, 9–15.

Hartong, D. T., Berson, E. L., & Dryja, T. P. (2006). Retinitis pigmentosa. *Lancet, 368*(9549), 1795–1809.

Hernowo, A. T., Boucard, C. C., Jansonius, N. M., Hooymans, J. M., & Cornelissen, F. W. (2011). Automated morphometry of the visual pathway in primary open-angle glaucoma. *Investigative Ophthalmology and Visual Science, 52*(5), 2758–2766.

Jiang, F., Stecker, G. C., Boynton, G. M., & Fine, I. (2016). Early blindness results in developmental plasticity for auditory motion processing within auditory and occipital cortex. *Frontiers in Human Neuroscience, 10*, 324.

Jiang, J., Zhu, W., Shi, F., Liu, Y., Li, J., Qin, W., et al. (2009). Thick visual cortex in the early blind. *Journal of Neuroscience, 29*(7), 2205–2211.

Jutras, M. J., & Buffalo, E. A. (2010). Synchronous neural activity and memory formation. *Current Opinion in Neurobiology, 20*(2), 150–155.

Kagan, I., Gur, M., & Snodderly, D. M. (2008). Saccades and drifts differentially modulate neuronal activity in V1: Effects of retinal image motion, position, and extraretinal influences. *Journal of Vision, 8*(14), 11–25.

Karlen, S. J., Kahn, D. M., & Krubitzer, L. (2006). Early blindness results in abnormal corticocortical and thalamocortical connections. *Neuroscience, 142*(3), 843–858.
Knyazeva, M. G., Fornari, E., Meuli, R., Innocenti, G., & Maeder, P. (2006). Imaging of a synchronous neuronal assembly in the human visual brain. *Neuroimage, 29*(2), 593–604.
Liu, X., Lin, X., Zheng, M., Hu, Y., Wang, Y., Wang, L., et al. (2018). Internet search alters intra- and inter-regional synchronization in the temporal gyrus. *Frontiers in Psychology, 9*, 260.
Liu, Y., Yu, C., Liang, M., Li, J., Tian, L., Zhou, Y., et al. (2007). Whole brain functional connectivity in the early blind. *Brain, 130*(Pt 8), 2085–2096.
Masuda, Y., Horiguchi, H., Dumoulin, S. O., Furuta, A., Miyauchi, S., Nakadomari, S., et al. (2010). Task-dependent V1 responses in human retinitis pigmentosa. *Investigative Ophthalmology and Visual Science, 51*(10), 5356–5364.
Nakamura, H. (2018). Cerebellar projections to the ventral lateral geniculate nucleus and the thalamic reticular nucleus in the cat. *Journal of Neuroscience Research, 96*(1), 63–74.
Neuenschwander, S., Castelo-Branco, M., Baron, J., & Singer, W. (2002). Feed-forward synchronization: Propagation of temporal patterns along the retinothalamocortical pathway. *Philosophical Transactions of the Royal Society of London. Series B, Biological Sciences, 357*(1428), 1869–1876.
Neuenschwander, S., & Singer, W. (1996). Long-range synchronization of oscillatory light responses in the cat retina and lateral geniculate nucleus. *Nature, 379*(6567), 728–732.
Nir, Y., Hasson, U., Levy, I., Yeshurun, Y., & Malach, R. (2006). Widespread functional connectivity and fMRI fluctuations in human visual cortex in the absence of visual stimulation. *Neuroimage, 30*(4), 1313–1324.
Ohno, N., Murai, H., Suzuki, Y., Kiyosawa, M., Tokumaru, A. M., Ishii, K., et al. (2015). Alteration of the optic radiations using diffusion-tensor MRI in patients with retinitis pigmentosa. *British Journal of Ophthalmology, 99*(8), 1051–1054.
Park, H. J., Lee, J. D., Kim, E. Y., Park, B., Oh, M. K., Lee, S., et al. (2009). Morphological alterations in the congenital blind based on the analysis of cortical thickness and surface area. *Neuroimage, 47*(1), 98–106.
Pipa, G., & Munk, M. H. (2011). Higher Order Spike Synchrony in Prefrontal Cortex during Visual Memory. *Frontiers in Computational Neuroscience, 5*, 23.
Ploner, M., Schmitz, F., Freund, H. J., & Schnitzler, A. (2000). Differential organization of touch and pain in human primary somatosensory cortex. *Journal of Neurophysiology, 83*(3), 1770–1776.
Ptito, M., Schneider, F. C., Paulson, O. B., & Kupers, R. (2008). Alterations of the visual pathways in congenital blindness. *Experimental Brain Research, 187*(1), 41–49.
Reislev, N. H., Dyrby, T. B., Siebner, H. R., Lundell, H., Ptito, M., & Kupers, R. (2017). Thalamocortical connectivity and microstructural changes in congenital and late blindness. *Neural Plast, 2017*, 9807512.
Rita Machado, A., Carvalho Pereira, A., Ferreira, F., Ferreira, S., Quendera, B., Silva, E., et al. (2017). Structure-function correlations in Retinitis Pigmentosa patients with partially preserved vision: A voxel-based morphometry study. *Scientific Reports, 7*(1), 11411.
Rizzolatti, G., & Matelli, M. (2003). Two different streams form the dorsal visual system: Anatomy and functions. *Experimental Brain Research, 153*(2), 146–157.
Rossetti, A., Miniussi, C., Maravita, A., & Bolognini, N. (2012). Visual perception of bodily interactions in the primary somatosensory cortex. *European Journal of Neuroscience, 36*(3), 2317–2323.
Sabbah, N., Authie, C. N., Sanda, N., Mohand-Said, S., Sahel, J. A., Safran, A. B., et al. (2016). Increased functional connectivity between language and visually deprived areas in late and partial blindness. *Neuroimage, 136*, 162–173.
Sabbah, N., Sanda, N., Authie, C. N., Mohand-Said, S., Sahel, J. A., Habas, C., et al. (2017). Reorganization of early visual cortex functional connectivity following selective peripheral and central visual loss. *Scientific Reports, 7*, 43223.
Sliwinska, M. W., James, A., & Devlin, J. T. (2015). Inferior parietal lobule contributions to visual word recognition. *Journal of Cognitive Neuroscience, 27*(3), 593–604.
Smith, R., Alkozei, A., Bao, J., Smith, C., Lane, R. D., & Killgore, W. D. S. (2017). Resting state functional connectivity correlates of emotional awareness. *Neuroimage, 159*, 99–106.
Song, X. W., Dong, Z. Y., Long, X. Y., Li, S. F., Zuo, X. N., Zhu, C. Z., et al. (2011). REST: A toolkit for resting-state functional magnetic resonance imaging data processing. *PLoS One, 6*(9), e25031.
Sturm, A. K., & Konig, P. (2001). Mechanisms to synchronize neuronal activity. *Biological Cybernetics, 84*(3), 153–172.
van der Togt, C., Kalitzin, S., Spekreijse, H., Lamme, V. A., & Super, H. (2006). Synchrony dynamics in monkey V1 predict success in visual detection. *Cerebral Cortex, 16*(1), 136–148.
Wang, K., Jiang, T., Yu, C., Tian, L., Li, J., Liu, Y., et al. (2008). Spontaneous activity associated with primary visual cortex: A resting-state FMRI study. *Cerebral Cortex, 18*(3), 697–704.
Wang, J., Li, T., Zhou, P., Wang, N., Xian, J., & He, H. (2017). Altered functional connectivity within and between the default model network and the visual network in primary open-angle glaucoma: A resting-state fMRI study. *Brain Imaging and Behavior, 11*(4), 1154–1163.
Wong, F., & Kwok, S. Y. (2016). The Survival of Cone Photoreceptors in Retinitis Pigmentosa. *JAMA Ophthalmol, 134*(3), 249–250.
Yu, C., Liu, Y., Li, J., Zhou, Y., Wang, K., Tian, L., et al. (2008). Altered functional connectivity of primary visual cortex in early blindness. *Human Brain Mapping, 29*(5), 533–543.
Zang, Y., Jiang, T., Lu, Y., He, Y., & Tian, L. (2004). Regional homogeneity approach to fMRI data analysis. *Neuroimage, 22*(1), 394–400.
Zhang, Y., Guo, X., Wang, M., Wang, L., Tian, Q., Zheng, D., et al. (2016). Reduced field-of-view diffusion tensor imaging of the optic nerve in retinitis pigmentosa at 3T. *AJNR American Journal of Neuroradiology, 37*(8), 1510–1515.
Zhang, J., Wang, C., Shen, Y., Chen, N., Wang, L., Liang, L., et al. (2016). A mutation in ADIPOR1 causes nonsyndromic autosomal dominant retinitis pigmentosa. *Human Genetics, 135*(12), 1375–1387.
Zuo, L., Wang, S., Yuan, J., Gu, H., Zhou, Y., & Jiang, T. (2017). Altered intra- and interregional synchronization in the absence of the corpus callosum: A resting-state fMRI study. *Neurological Sciences, 38*(7), 1279–1286.
Zuo, X. N., Xu, T., Jiang, L., Yang, Z., Cao, X. Y., He, Y., et al. (2013). Toward reliable characterization of functional homogeneity in the human brain: Preprocessing, scan duration, imaging resolution and computational space. *Neuroimage, 65*, 374–386.